ACS OMEGA

http://pubs.acs.org/journal/acsodf

Article

Liposomal Delivery of MicroRNA-7 Targeting EGFR to Inhibit the Growth, Invasion, and Migration of Ovarian Cancer

Xiaojuan Cui, Keqi Song, Xiaolan Lu, Weiwei Feng,* and Wen Di*

Cite This: *ACS Omega* 2021, 6, 11669−11678

Read Online

ACCESS | Metrics & More | Article Recommendations

ABSTRACT: Ovarian cancer is highly aggressive and has high rates of recurrence and metastasis. Due to the limited effects of current treatments, it is necessary to conduct research and develop new treatment options. The application of gene therapy in tumor therapy is gradually increasing and has exciting prospects. MicroRNA-7 (miR-7) has been reported to inhibit the growth, invasion, and metastasis of a variety of solid tumors. Cationic liposomes are safe and effective gene delivery systems for transfection in vivo and in vitro. To realize the application of miR-7 in the treatment of ovarian cancer, cationic liposomes were prepared with 1,2-dioleoyl-3-trimethylammonium-propane, 1,2-dioleoyl-*sn*-glycero-3-phosphoethanolamine, and cholesterol. The miR-7 liposomes had a suitable particle size, potential, and a high cellular uptake rate. MiR-7 encapsulated by liposomes could be effectively delivered to ovarian cancer cells and successfully targeted to the tumor site in a mouse xenograft model of ovarian cancer. In vitro and in vivo experiments revealed that the miR-7 liposomes had a significant ability to inhibit the growth, invasion, and migration of ovarian cancer, probably by inhibiting the expression of the epidermal growth factor receptor. Our studies of miR-7 liposomes demonstrated a safe and efficient microRNA delivery system for the gene therapy of ovarian cancer.

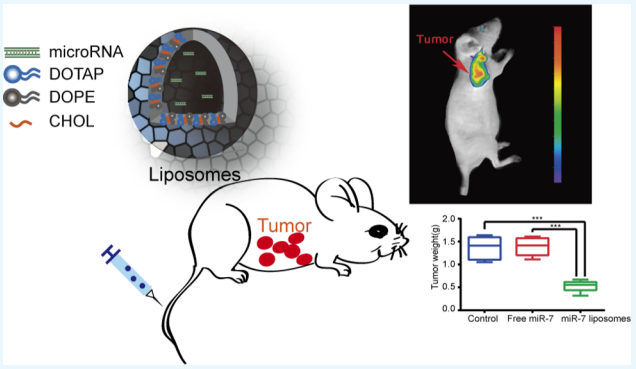

INTRODUCTION

The incidence of ovarian cancer ranks third among gynecological malignancies worldwide. It is worth noting that ovarian cancer is the most lethal gynecological malignant neoplasm.[1] Although optimal cytoreduction, chemotherapy, and maintenance therapy with polyadenosine diphosphate ribose polymerase inhibitors, bevacizumab, or drugs targeting homologous recombination deficiency have improved the quality of life of some patients, most patients with ovarian cancer still experience recurrence and metastasis. The treatment of recurrent and metastatic ovarian cancer is more difficult than the initial ovarian cancer, and it is worthy of further study.[2]

In recent years, gene therapy has been extensively studied and applied. In the field of vaccines, RNA has been used to develop vaccines against the coronavirus that has swept the world.[3] In the field of oncology, DNA, RNA, and oligonucleotides are used to silence oncogenes, correct gene mutations, or introduce genes that inhibit tumor growth, invasion, and metastasis.[4] In many reports, microRNA-7 (miR-7) has been shown to have an inhibitory effect on tumor growth, invasion, and metastasis. The epithelial−mesenchymal transition and invasiveness of glioblastoma multiforme could be repressed by miR-7 through T-Box 2.[5] The growth and metastasis of osteosarcoma cells could be inhibited by miR-7 through IGF1R.[6] MiR-7 regulates the growth and invasiveness of sorafenib-resistant cells in human hepatocellular carcinoma.[7] Importantly, miR-7 in exosomes may inhibit the metastasis of ovarian cancer cells by inhibiting the EGFR/AKT/ERK1/2 pathway.[8] Our previous studies have shown that the combination of miR-7 and paclitaxel encapsulated by polymers (mPEG−PLGA−PLL) enhanced ovarian cancer cell chemotherapy sensitivity, and this effect might be mediated by the inhibition of the EGFR/ERK pathway.[9] However, the tumor suppressor effect of miR-7 alone has not been studied in depth in ovarian cancer.

The application of miR-7 in the treatment of ovarian cancer is facing some challenges. Naked miR-7 is easily degraded by RNases in the extracellular space or the bloodstream and it lacks biomembrane permeability.[10] Viral vectors that are often used as the gene transfection tools possess the possibility of random integration into the host genome. This may cause

Received: February 23, 2021
Accepted: April 6, 2021
Published: April 19, 2021

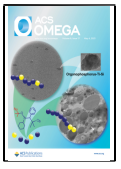

https://doi.org/10.1021/acsomega.1c00992
ACS Omega 2021, 6, 11669−11678

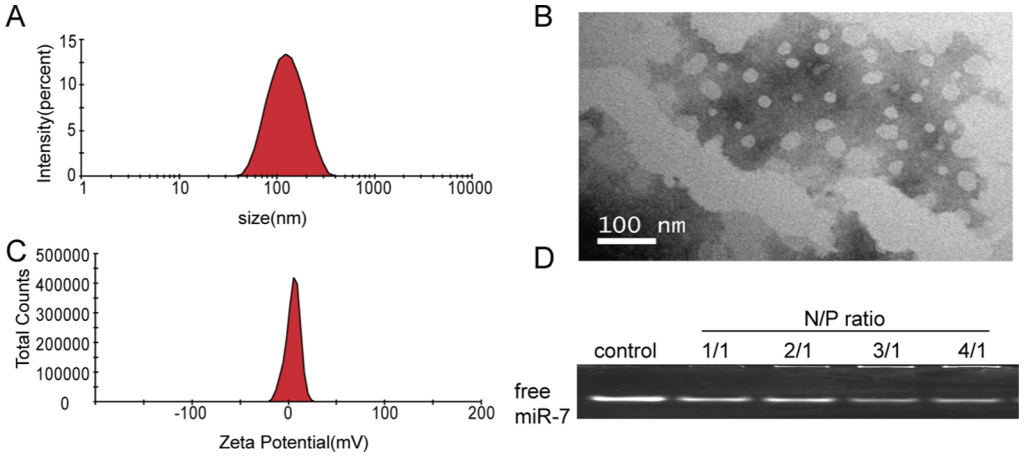

Figure 1. Characterization of miR-7 liposomes. (A) Particle distribution of the miR-7 liposomes. (B) TEM image of the miR-7 liposomes. (C) ζ potential of miR-7 liposomes showing a positive charge. (D) Free miR-7 under different N/P ratios detected by agarose gel electrophoresis.

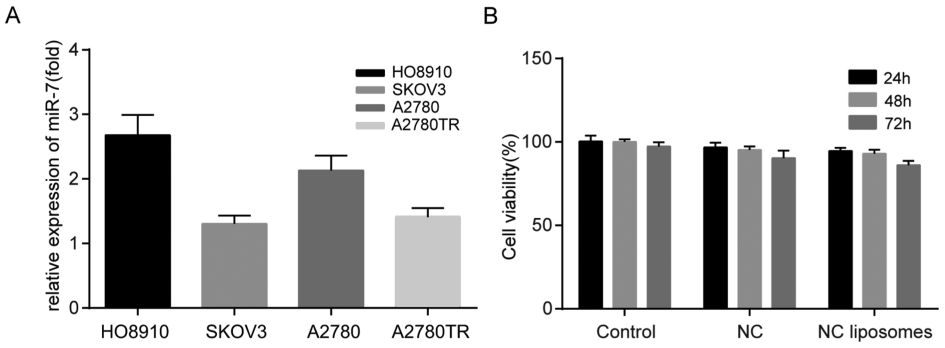

Figure 2. Comparison of the miR-7 content in the ovarian cancer cell lines and detection of unloaded liposome toxicity. (A) Comparison of the miR-7 content in the ovarian cancer cell lines HO8910, SKOV3, A2780, and A2780TR. (B) Cell viability of SKOV3 cells incubated with NC liposomes for 24, 48, and 72 h. The error bars represent ±SD.

mutations and stimulate strong immunogenicity, so the use of viral vectors is greatly restricted.[11] In recent years, cationic liposomes have received widespread attention in the preparation of genetic drugs. Cationic liposomes are simple to prepare and highly stable. They can easily encapsulate negatively charged nucleic acids and have high loading efficiency and low cytotoxicity.[12] Cationic lipids are the basis for the preparation of cationic liposomes. We chose 1,2-dioleoyl-3-trimethylammonium-propane (DOTAP), which is commonly used in research. Zwitterionic lipid 1,2-dioleoyl-*sn*-glycero-3-phosphoethanolamine (DOPE) is often used to prepare liposomes together with cationic lipids, so it is also known as the helper lipid. This kind of helper lipid can stabilize the bilayer membrane and reduce the toxicity of the positive components. DOPE interferes with the lipid membrane, makes the endosomal membrane unstable, and promotes the release of its cargo of DNA or RNA into the cell. At the same time, DOPE assists cationic liposome cell permeability and significantly improves the transmembrane efficiency.[13] In addition, cholesterol (CHOL) can also adjust the fluidity of phospholipid bilayer membranes, reduce membrane permeability, and reduce drug leakage.[14] Because PEG may inhibit the interaction between gene carriers and the surface of tumor cells, affect the cell uptake of gene carriers,[15] and has a certain immunogenicity,[16] we did not add PEG while preparing the liposomes in this study. Consequently, we herein used DOTAP, DOPE, and CHOL to prepare liposomes to encapsulate and deliver miR-7 for in vivo and in vitro experiments in ovarian cancer. We hypothesized that miR-7 could successfully target the tumor site through liposome transfection and inhibit the growth, invasion, and migration of ovarian cancer cells by inhibiting the epidermal growth factor receptor (EGFR). The characteristics, toxicity, targeting, tumor suppressor effect, and inhibition of EGFR by miR-7 liposomes were explored both in vivo and in vitro for ovarian cancer.

RESULTS AND DISCUSSION

Characterization of the Liposomes. To understand the physical properties of the liposomes, we measured their particle size and ζ potential. The data showed that the particle sizes and zeta potentials of the liposomes were 127.43 ± 0.41 nm and +9.23 ± 0.67 mV, with a polydispersity index of 0.165 ± 0.004 (Figure 1A, C). With a quaternary ammonium head group, DOTAP is a commonly used cationic lipid for gene transfection. In a wide pH range, DOTAP is positively charged.[17] Therefore, the above liposomes have a certain positive charge to attract negatively charged mRNA. Importantly, an excessive positive charge will produce greater cytotoxicity, and cationic DOTAP liposomes alone have poor stability,[4] so we added a certain proportion of DOPE and CHOL when preparing the liposomes. The two aliphatic tails of DOPE each contain a cis double bond. Because of its ability to stabilize lipid bilayer membranes and reduce the toxicity of cationic lipids, DOPE is a frequently used helper lipid.[18] CHOL also has a good stabilizing effect on the bilayer membrane structure of the liposomes.[19]

https://doi.org/10.1021/acsomega.1c00992
ACS Omega 2021, 6, 11669−11678

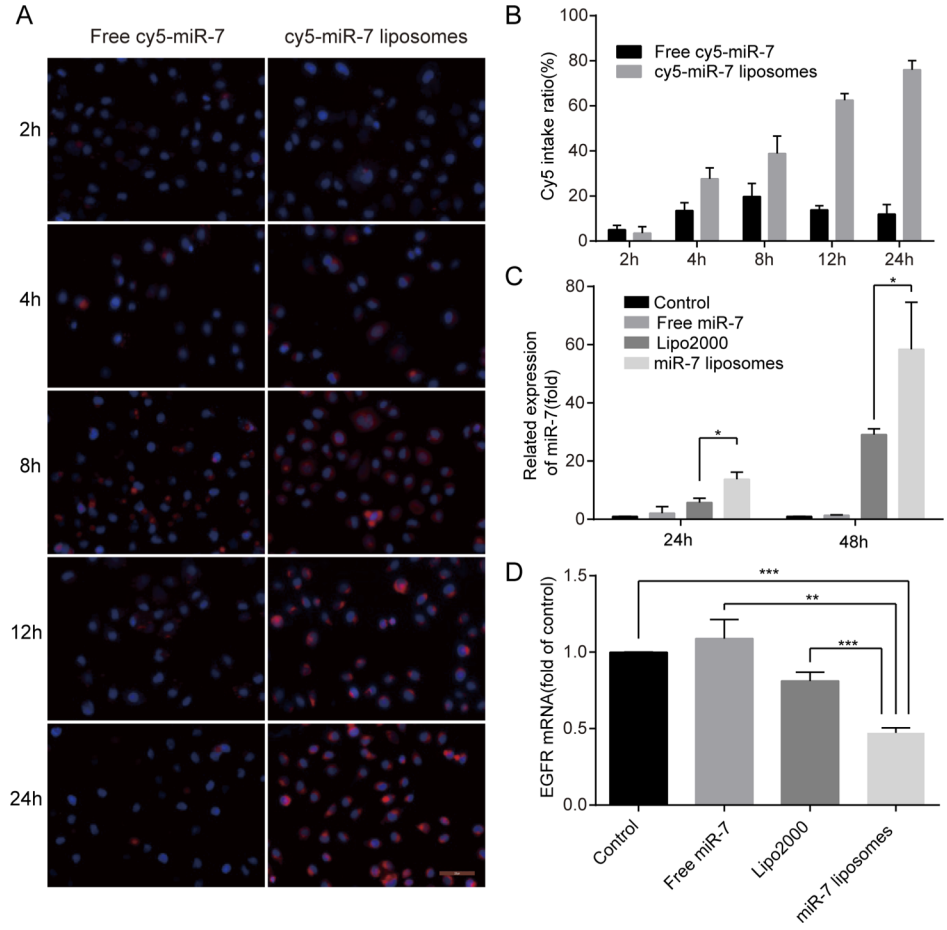

Figure 3. In vitro cellular uptake, transfection efficiency, and inhibition rate of EGFR mRNA in miR-7 liposomes. (A) Images of SKOV3 cells incubated with free cy5-miR-7 or cy5-miR-7 liposomes after 4, 8, 12, and 24 h by fluorescence microscopy (the scale bar is 200 μm). (B) Quantification of the Cy5 fluorescence intake ratio of (A). (C) Transfection efficiency of the miR-7 liposomes in SKOV3 cells compared with PBS, free miR-7, and Lipo2000 at a miR-7 dose of 100 nM. (D) Inhibition rate of EGFR mRNA of miR-7 liposomes in SKOV3 cells compared with PBS, free miR-7, and Lipo2000 at a miR-7 dose of 100 nM (n = 3). The error bars represent ±SD; Student's t-test was performed for statistical analysis; *p < 0.05, **p < 0.01, and ***p < 0.001.

To show the shape of the liposomes, we took a picture with a transmission electron microscope (TEM). The liposomes presented a stable round-like morphology at a size of approximately 100 nm with good dispersion by TEM (Figure 1B). In the experiment, we used phosphate-buffered saline (PBS) as the solvent when preparing liposomes by the thin-film dispersion method. There are also some studies suggesting that PBS medium can enhance the stability of liposomes.[13]

The ability of liposomes to carry RNA is mainly related to the ratio of DOTAP, DOPE, CHOL, and the cell types.[20] According to the literature and orthogonal experiments, the ratio in our experiment is DOTAP/DOPE/CHOL = 1:1:0.25. To demonstrate the best encapsulation rate of miR-7 and the appropriate N/P ratio, agarose gel electrophoresis was used to determine the content of free miR-7 under different N/P ratios. We found that when the N/P ratio reached 4/1, only a few free miR-7 molecules were observed (Figure 1D). This finding indicates that N/P = 4/1 is an appropriate ratio, and the encapsulation rate of RNA is higher at this ratio. Some related studies have also described similar N/P ratios,[21,22] so we used this ratio (4/1) to prepare miR-7 liposomes in all subsequent experiments.

Detection of miR-7 in the Ovarian Cancer Cell Lines. To select a suitable experimental ovarian cell line, we used TaqMan miRNA assays to detect the content of miR-7 in HO8910, SKOV3, A2780, and A2780TR cells. We found that the content of miR-7 in the ovarian cancer cell line SKOV3 was the lowest compared with the other cell lines (Figure 2A). Studies have shown that EGFR is one of the target proteins of miR-7 and that miR-7 potently suppresses tumor cell proliferation by inhibiting the EGFR pathway.[23] The EGFR expression in SKOV3 cells was also higher than in the other ovarian cancer cell lines.[24] Therefore, we chose SKOV3 for the follow-up in vitro experiments, and the expression of tumor EGFR was further detected after the transfection of miR-7.

Toxicity Test of the Unloaded Liposomes. The toxicity of cationic liposomes has always been an issue that needs attention.[25] To prove the safety of the liposomes, NC liposomes were prepared and incubated with SKOV3 cells for 24, 48, and 72 h. As shown in Figure 2B, after 72 h of incubation with NC liposomes, the activity of the SKOV3 cells was still as high as 86.0 ± 2.69%. The data indicate that the liposomes exhibited negligible cytotoxicity and could be used as gene carriers for in vivo and in vitro experiments.

In Vitro Uptake and Transfection Efficiency of the Liposomes. To demonstrate the cellular uptake of the liposomes, cy5-miR-7 liposomes were prepared and incubated with SKOV3 cells for 2, 4, 8, 12, and 24 h. We found that the

https://doi.org/10.1021/acsomega.1c00992
ACS Omega 2021, 6, 11669−11678

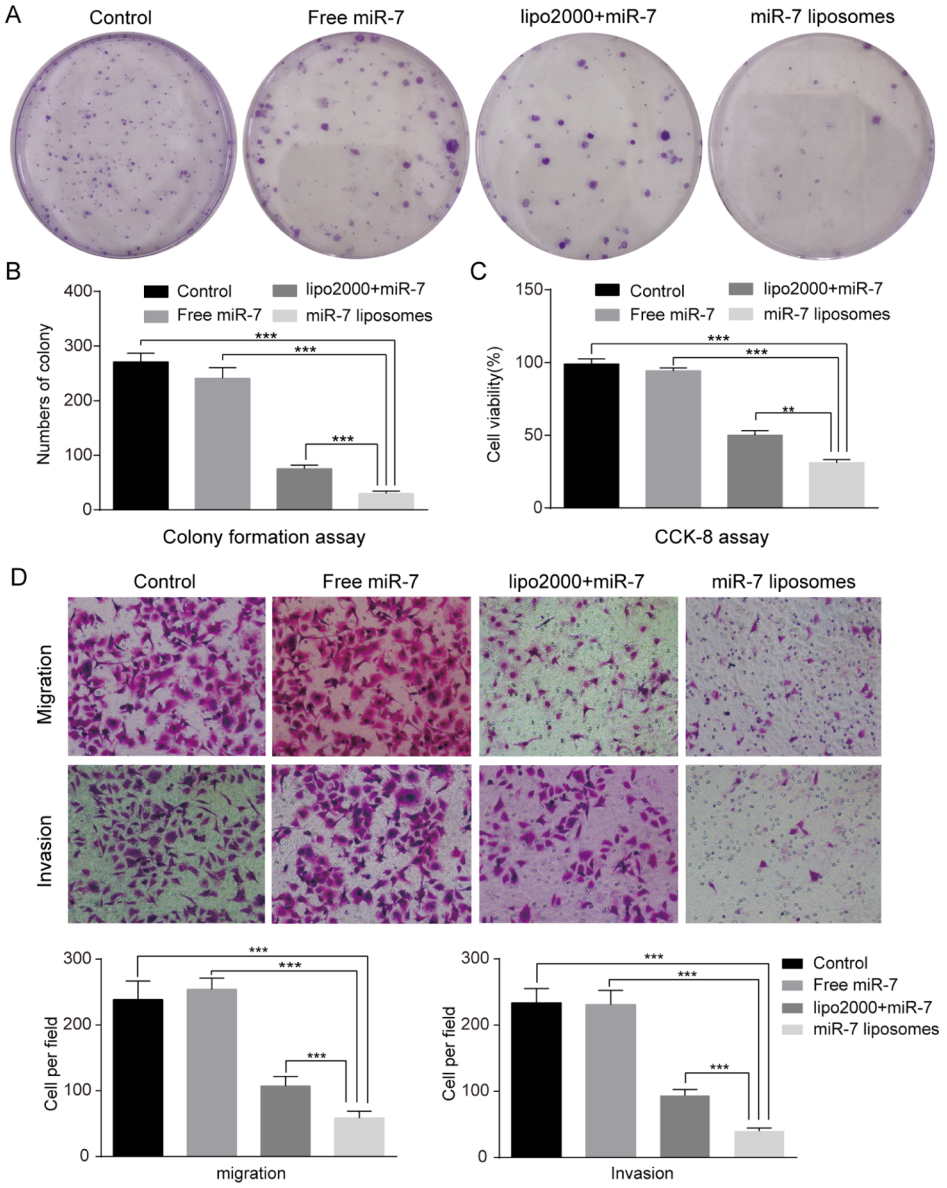

Figure 4. miR-7 liposomes inhibited SKOV3 cell proliferation, invasion, and migration. (A) Images showing the clonogenic ability of SKOV3 cells following treatment with PBS, free miR-7, Lipo2000 + miR-7, and miR-7 liposomes at a miR-7 dose of 100 nM. (B) Quantification of the SKOV3 colonies of (A). (C) Cell viability of the SKOV3 cells following treatments with PBS, free miR-7, Lipo2000 + miR-7, and miR-7 liposomes at a miR-7 dose of 100 nM after 72 h. (D) Migration and invasion assays showed that miR-7 liposomes had the strongest inhibitory effect on the invasion and migration abilities of SKOV3 cells compared with the control group, free miR-7 group, and Lipo2000 + miR-7 group at a miR-7 dose of 100 nM. The error bars represent ±SD; Student's *t*-test was performed for statistical analysis; $*p < 0.05$, $**p < 0.01$, and $***p < 0.001$.

cellular uptake rate of free cy5-miR-7 within 2 to 24 h was very low, while cy5-miR-7 liposomes had an obvious uptake by SKOV3 after 2 h. Over time, the uptake rate of the liposomes increased. After 24 h of incubation, the uptake rate of the liposomes reached more than 75% (Figure 3A,B). Therefore, we next explored the transfection efficiency of miR-7 liposomes in SKOV3 cells by TaqMan miRNA assays. The results showed that 24 h after transfection of miR-7 liposomes, the transfection rate was improved compared with that of Lipo2000. After 48 h, the difference was even more obvious. The related expression of miR-7 in the Lipo2000 group increased by 29 times on average, while that in the miR-7 liposome group increased by 58 times (Figure 3C). Compared with the previous literature,[26] our prepared miR-7 liposomes composed of DOTAP, DOPE, and CHOL have a higher transfection efficiency. Compared with the polymer nanoparticles prepared by our team,[9] the transfection ability of miR-7 liposomes is higher. This greater ability may be related to using the proper ratio of liposome components, and liposomes have a better carrying capacity for miR-7. Next, we detected the changes in EGFR mRNA, one of the miR-7 target genes, after cell transfection. The data showed that the inhibition rate of EGFR mRNA in the miR-7 liposome group reached more than 50%, which was statistically significant compared with the Lipo2000 group (Figure 3D). Based on the above results, the miR-7 liposomes could be effectively taken up by SKOV3 and could exert a high transfection efficiency, and significantly reduce the expression of target RNA. To further confirm these results, in subsequent in vitro experiments, the transfection efficiency of miR-7 liposomes will be further confirmed.

https://doi.org/10.1021/acsomega.1c00992
ACS Omega 2021, 6, 11669−11678

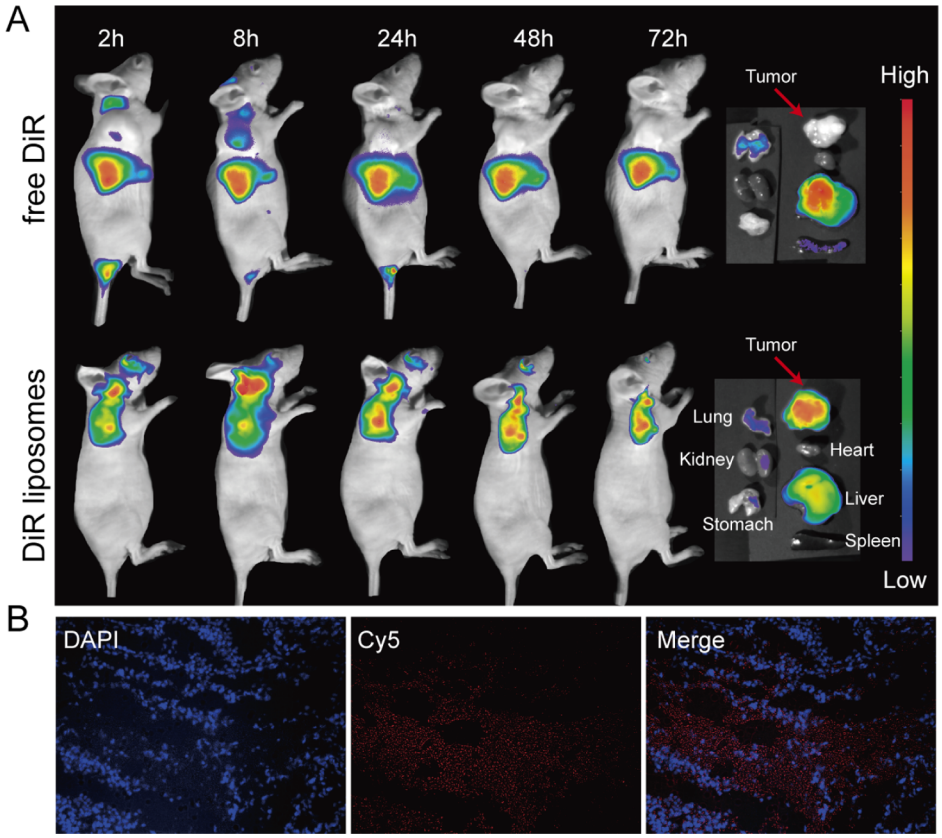

Figure 5. Distribution of liposomes in the mouse subcutaneous xenograft model. (A) Fluorescence images of mice demonstrated that only a small amount of the drug was observed in the tumor site at 2 h and 8 h in the free DiR group. However, fluorescence was clearly observed in the tumor sites at 2, 8, 24, 48, and 72 h in the DiR liposome group. From the right to left and from the top to bottom, the fluorescence images of the tumors, hearts, livers, spleens, lungs, kidneys, and stomachs on the far right show that the fluorescence in the DiR liposome group was mainly focused at the tumor site. (B) Fluorescence images of frozen tumor slices at 24 h after the injection of cy5-miR-7 liposomes. The blue fluorescence represents the nucleus after 4′,6-diamidino-2-phenylindole (DAPI) staining; the red fluorescence represents cy5-miR-7.

Cytotoxicity Study of SKOV3. To prove the inhibitory ability of miR-7 liposomes on proliferation, we conducted colony formation assays and CCK-8 experiments. The results of clone formation experiments suggested that miR-7 liposomes had a more obvious inhibitory effect on the clonogenic ability of SKOV3 cells than Lipo2000 (Figure 4A,B). Next, we examined the effect of the inhibitory ability of miR-7 liposomes on proliferation by CCK-8. We found that after miR-7 liposomes interacted with SKOV3 cells for 72 h, the cell viability decreased to 31% (Figure 4C). Our previous studies on the ovarian cancer cell line HO8910pm using high-molecular weight polymers to transfect miR-7 showed that miR-7 has a limited inhibitory effect on cell proliferation.[9] However, the research using SKOV3 suggested that miR-7 suppressed the proliferation of SKOV3 cells, and the growth inhibitory effect was enhanced by liposome transfection. This apparent discrepancy could be explained by differences in cell types and transfection efficiency. The SKOV3 cells we chose are highly invasive and have a low miR-7 content. Studies have reported that miR-7 inhibits the motility and wound healing potential of breast cancer cells, especially in highly aggressive cell lines. Moreover, miR-7 inhibited the proliferation, invasion and migration of endothelial cells, which is an important condition for tumor invasion.[27] Other research also suggested that miR-7 potently suppressed the proliferation of colorectal cancer cells and that EGFR is a direct target of miR-7.[23] As mentioned above, miR-7 liposomes have a certain inhibitory effect on the proliferation of SKOV3 cells.

Migration and Invasion Assay. Many studies have shown that EGFR enhances the migration, invasion, and metastasis of tumor cells. According to the previous reports, EGFR is related to tumorigenesis, invasion, and metastasis of lung cancer[28] and liver cancer.[29] To study whether the increase in miR-7 and the decrease in EGFR had an effect on the migration and invasion of SKOV3 cells, we conducted subsequent Transwell experiments. The results suggested that after miR-7 transfection, the migration and invasion abilities of SKOV3 cells were significantly inhibited, especially in the miR-7 liposome treatment group. Compared with the control group, the inhibition rates of migration and invasion in the miR-7 liposome group reached 70.2 and 75.3%, respectively (Figure 4D). Some previous studies also suggested that a direct or indirect increase in miR-7 in ovarian cancer cells significantly inhibited tumor invasion and metastasis.[8,30] Our results confirmed that the high-efficiency transfection of miR-7 in vitro could significantly inhibit the motility of SKOV3 cells, and the inhibition rate was slightly higher than that previously reported in the literature.

Distribution of Liposomes in the Mouse Subcutaneous Xenograft Model. To prove the tumor-targeting effect of liposomes in vivo, 1,1′-dioctadecyl-3,3,3′,3′-tetramethylindotricarbocyanine iodide (DiR) liposomes were prepared and intravenously injected into tumor-bearing mice. At 2, 8,

https://doi.org/10.1021/acsomega.1c00992
ACS Omega 2021, 6, 11669−11678

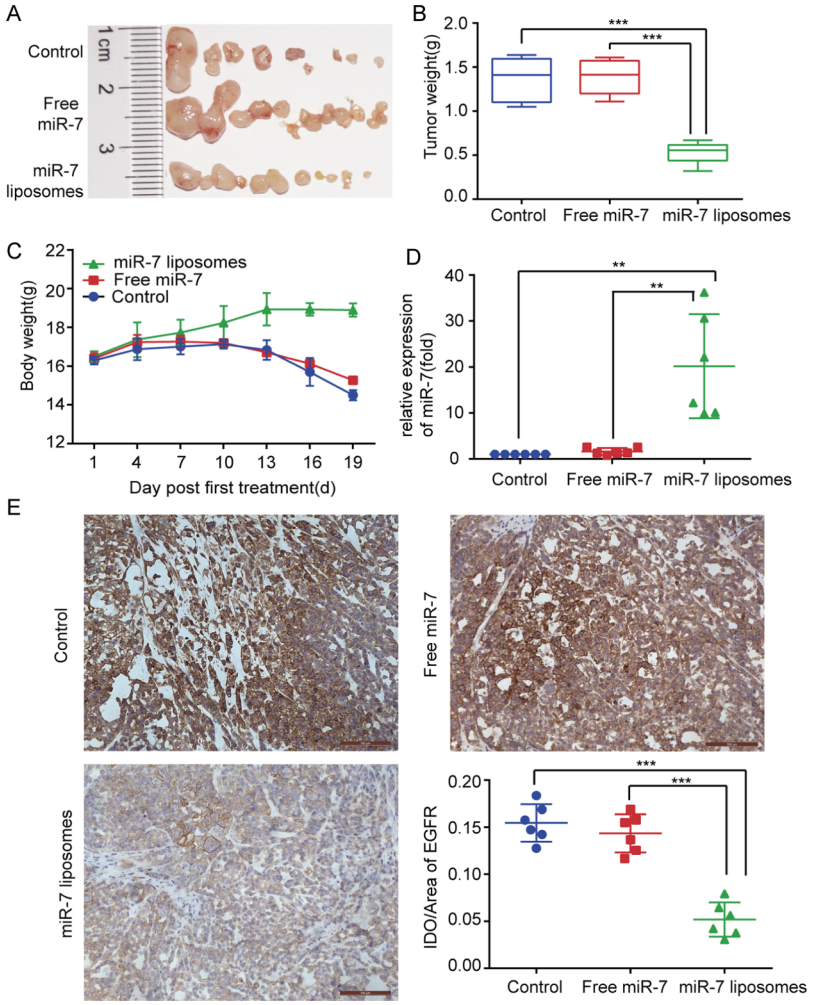

Figure 6. Antitumor efficiency of miR-7 liposomes in a mouse abdominal cavity xenograft model and EGFR inhibition. (A) Photographs of the abdominal tumors in the control, free miR-7, and miR-7 liposome groups. (B) Comparison of the tumor weights shows that the miR-7 liposome treatment group had the smallest tumor burden. (C) Changes in the body weight of the mice in each group. (D) Comparison of the miR-7 content of tumors in each group reflects the higher transfection efficiency of miR-7 liposomes in mice. (E) Immunohistochemistry of tumors showed that the EGFR expression in the miR-7 liposome treatment group was significantly decreased (scale bar: 100 μm). The error bars represent ±SD; Student's *t*-test was performed for statistical analysis; *$p < 0.05$, **$p < 0.01$, and ***$p < 0.001$.

24, 48, and 72 h after injection, the mice were placed under an in vivo imaging system to take images. The images revealed that in the free DiR group, only a small amount of the drug was observed in the tumor site at 2 and 8 h, and no drug was observed in the tumor site at 24, 48, and 72 h. However, in the DiR liposome group, obvious fluorescence was observed in the tumor site at 2, 8, 24, 48, and 72 h. After 72 h, the subcutaneous tumors, hearts, livers, spleens, lungs, kidneys, and stomachs of the two groups of mice were removed for observation. The fluorescence in the free DiR group was mainly concentrated in the livers and lungs, and no obvious fluorescence was observed at the tumor site. The fluorescence in the DiR liposome group was mainly focused at the tumor site and only a small amount of fluorescence was seen in the livers and lungs (Figure 5A).

Then, we wanted to further determine whether miR-7 could successfully enter the tumor tissue by liposome delivery. Cy5-miR-7 liposomes were prepared and injected into mice through the tail vein. After 24 h, frozen slices of the tumors were obtained. A large amount of red fluorescence displayed by cy5-miR-7 in the tumor tissue was observed by a fluorescence microscope (Figure 5B). This finding indicates that miR-7 could be successfully delivered by liposomes to the tumor. Combined with our research results and literature reports, the tumor-targeting properties of liposomes might be related to the enhanced retention and permeability effect[31] of the nanoparticles and the transcytosis of the tumor endothelial cells.[32] Little is currently known about the transcytosis process.[33] Recent studies have suggested that the positive charge of nanoparticles might promote transcytosis.[34] Therefore, the cationic liposomes used in this study might partially enhance their tumor-targeting effects, but the specific mechanism needs to be further studied in the future.

Antitumor Efficiency of MiR-7 Liposomes in a Mouse Abdominal Cavity Xenograft Model. SKOV3 cells were implanted into the abdominal cavity of the mice to construct a mouse abdominal cavity xenograft model. We wanted to use this animal model to simulate the widespread metastasis of ovarian cancer in the peritoneal cavity. As shown in Figure 6A,B, compared with the other treatment groups, the abdominal tumor burden in the miR-7 liposome treatment groups was significantly decreased, and the total weight of the

https://doi.org/10.1021/acsomega.1c00992
ACS Omega 2021, 6, 11669−11678

tumor was also significantly reduced. To evaluate the in vivo toxicity of the miR-7 liposomes, we recorded the body weight changes of the mice. The body weight is also one of the values of the disease score in cancer. The results showed that the weight of the mice in the miR-7 liposome treatment group did not significantly decrease, while the weight of the mice in the control group had a tendency to decrease (Figure 6C). This indicated that miR-7 liposomes had no significant impact on the weight of the mice, and the weight loss of the control group might be caused by the excessive tumor burden and the excessive body tissue consumption caused by tumor cachexia.

To determine the liposome transfection efficiency in mice, the miR-7 content of the abdominal tumors was tested. The data showed that the content of miR-7 in the free miR-7 treatment group was similar to that of the control group, but the intratumoral miR-7 content in the miR-7 liposome treatment group was 20.9-fold that in the control group (Figure 6D). These data once again showed that miR-7 could be efficiently delivered to the tumor site by liposomes.

Some recent research reports have suggested the tumor suppressor effect of miR-7 in vivo. For example, after transfection with lentivirus, breast cancer stem cells highly expressed miR-7. The tumor-forming ability of these stem cells in mice was significantly weakened.[35] After the application of miR-7 mimics in a mouse model of orthotopic transplantation of osteosarcoma, the tumor mass was significantly reduced, and the lung metastasis of osteosarcoma was also delayed and reduced.[6] However, in these studies, since free miR-7 is easily degraded, it was difficult to effectively use miR-7 in vivo. Liposomes are simple to synthesize, easy to use in vivo, and do not usually cause allergic reactions.[36] In our experiments, the effective function of miR-7 might be mainly attributed to the protection and transport of cationic liposomes.

In the in vitro experiments, we confirmed that EGFR mRNA could be significantly inhibited by miR-7. To further verify this result in vivo, an immunohistochemistry experiment was conducted to detect the expression of the EGFR protein in the tumor tissues. We noticed that the expression of the EGFR protein in the miR-7 liposome treatment group was significantly reduced by 64% compared with that in the free miR-7 treatment group (Figure 6E). Thus, at the current time, we have evidence that miR-7 could significantly inhibit the tumor EGFR protein expression. The EGFR pathway is closely related to tumor occurrence, development, invasion, and metastasis.[23] Therefore, miR-7 might have a tumor suppressor effect by inhibiting the EGFR pathway.

EXPERIMENTAL (MATERIALS AND METHODS)

Materials. For this study, DOTAP, DOPE, and CHOL were purchased from Avanti Polar Lipids, Inc. miR-7- and cy5-labeled miR-7 of the following sequence 5′-UGGAAGACUAGUGAUUUUGUUGU-3′ were obtained from Ruibo Biotechnology Inc (China). DiR was obtained from Biotium (Hayward). Cell counting kit-8 (CCK-8) was obtained from Dojindo (China). The anti-EGF receptor (D38B1) XP rabbit mAb #4267 was obtained from Cell Signaling Technology (MA). The quick-start protocol RNeasy Mini Kit was purchased from QIAGEN. Other materials were purchased from Sigma-Aldrich (St. Louis, MO) and used as obtained.

SKOV3, the human ovarian cancer cell line, was purchased from the Cell Bank of the Chinese Academy of Sciences (Shanghai, China). Cells were cultured in DMEM (HyClone, UT) containing 1% (v/v) penicillin/streptomycin (Sigma-Aldrich, MO) and 10% (v/v) fetal bovine serum (FBS) (Gibco, USA) in a thermostatic humidified cell CO_2 incubator at 37 °C.

Female BALB/c nude mice at 4−6 weeks of age were raised in specific pathogen-free conditions and purchased from the Chinese Academy of Sciences (Shanghai, China).

Preparation and Characterization of miR-7 Liposomes. With a molar proportion of 1:1:0.25, we dissolved DOTAP, DOPE and CHOL in a mixture of 3 ml chloroform and methanol. The mixture was evaporated by rotary evaporation at 37 °C for 30 min in a water bath and dried under vacuum for 8 h after film formation. The film was swollen in PBS solution. The PBS solution was obtained by dissolving the PBS powder in RNase-free water. The suspension was sonicated at 50 W for 3 min in a water bath and sonicated at 100 W for 3 min in an ice bath using an ultrasonic processor. After the suspension was extruded through 200 nm polycarbonate films, liposomes were obtained and stored at 4 °C.

MiR-7 was dissolved in RNase-free water before use. After incubating the liposomes and miR-7 at room temperature in a certain N/P ratio for 30 min, miR-7 liposomes were obtained. The ratio of N/P was calculated according to the following formula: DOTAP molecules in liposomes (amines-N)/negatively charged groups in microRNAs (phosphates—P). The phosphate content in miR-7 was 46 mol phosphates/mol miR-7.

The size and ζ potential of the miR-7 liposomes were measured by a Nano Zetasizer (Malvern, UK). The liposomes were observed under TEM to detect their morphology. The liposomes and miR-7 were mixed according to different N/P ratios. To identify the proper N/P ratio, the free RNA content in the miR-7 liposomes was determined by 1% (w/v) agarose gel electrophoresis.

Cell Line Selection. HO8910, SKOV3, A2780, and A2780TR (Taxol resistant) ovarian cancer cells were incubated at a density of 5×10^5 cells/well in six-well plates. To select the suitable ovarian cancer cell lines for the experiments, we extracted RNA from different cells with an RNeasy Mini Kit. Reverse transcription of miR-7 was performed by specific reverse transcription primers. cDNA was quantified via a TaqMan probe using TaqMan miRNA assays (Applied Biosystems, Foster City, CA). Human snRNA RNU6B (U6) was the internal loading control.

Cytotoxicity Assessment of the Unloaded Liposomes. We seeded SKOV3 cells in 96-well plates at a density of 5×10^3 cells per well. PBS, the free negative control RNA (NC), and NC liposomes were incubated with the cells for 24, 48, and 72 h. After the medium containing CCK-8 was reacted with the cells for 2 h, the optical density value was measured by a microplate reader. Then, the viability of the SKOV3 cells was calculated by GraphPad Prism 6.0 (CA, USA).

In Vitro Uptake and Transfection Efficiency of the Liposomes. SKOV3 cells were incubated in six-well plates (5×10^5 cells/well). To make the liposomes visible, we used cy5-labeled miR-7 to prepare Cy5-miR-7 liposomes. SKOV3 cells were incubated with the cy5-miR-7 liposomes for 2, 4, 8, 12, and 24 h. Free cy5 miR-7 was used as the control. Next, the medium was removed, and the cells were gently washed with PBS. After DAPI staining, the cells were observed by fluorescence microscopy (Nikon, Japan).

To test the transfection efficiency of the liposomes, SKOV3 cells were incubated with liposomes for 48 h. The control

https://doi.org/10.1021/acsomega.1c00992
ACS Omega 2021, 6, 11669−11678

groups were transfected with PBS, free miR-7, and Lipo2000 + miR-7 (positive control). The transfection concentration of miR-7 in each group was 100 nM. Then, the total RNA of the cells was extracted by an RNeasy Mini kit (Qiagen, Germany), and the miR-7 was detected by TaqMan miRNA assays. The level of EGFR mRNA in the cells was measured by RT-PCR using the PrimeScript reverse transcription reagent kit (TaKaRa Bio, China) and the SYBR Premix Ex Taq kit (TaKaRa Bio, China). The result was calculated using the $2^{-\Delta\Delta Ct}$ method.

In Vitro Cytotoxicity Assays of the miR-7 Liposomes. To observe the effect of miR-7 liposomes on the cell colony formation, we seeded SKOV3 cells in six-well plates at a density of 500 cells per well in triplicate. PBS, free miR-7, lipo2000 + miR-7 (positive control), and miR-7 liposomes were added to the medium (100 nM). Every 3 days, the culture medium was changed. After 2 weeks, the colonies were fixed with 4% paraformaldehyde and then stained with 0.5% crystal violet. The number of colonies was counted via an optical microscope.

To detect the effect of miR-7 liposomes on cell viability, we seeded SKOV3 cells in 96-well plates at a density of 5×10^3 cells per well. PBS, free miR-7, lipo2000 + miR-7, and miR-7 liposomes were added to the medium (miR-7 100 nM). The cell viability of the SKOV3 cells was measured by CCK-8 after 3 days. To further study the effect of miR-7 liposomes on proliferation, we seeded SKOV3 cells in 96-well plates at a density of 5000 cells per well in triplicate. PBS, free miR-7, lipo2000 + miR-7, and miR-7 liposomes were incubated with the cells for three days, and the viability was measured via CCK-8.

Migration and Invasion Assay. To perform the cell migration assay, PBS, free miR-7, lipo2000 + miR-7, and miR-7 liposomes containing 100 nM miR-7 were added to the serum-free RPMI-1640 medium. Then, SKOV3 cells were suspended in the appropriate medium. The cell suspensions were placed in the top chamber of a Transwell insert containing a polycarbonate membrane with an 8 mm pore size (Corning Costar, MD, USA). To perform the cell invasion assay, the Transwell inserts were pre-covered with 50 ml of the Matrigel matrix. RPMI-1640 medium containing 10% FBS was placed in the lower chamber as a chemoattractant. Twenty-four hours later, 0.1% crystal violet was used to stain the cells that had migrated or invaded through the membranes. Then, the cells were observed by a microscope.

In Vivo Imaging. To observe the in vivo tumor-targeting effect, a mouse subcutaneous xenograft model was constructed. We injected SKOV3 cells subcutaneously into the right forelimb of the mice at a cell number of 2.5×10^6. When the tumor volume reached approximately 200 mm^3 (tumor volume = $(\text{width}^2 \times \text{length})/2$), we randomly divided the mice into two groups. To facilitate the observation of the liposome distribution under an animal imaging system, a lipophilic, near-infrared fluorescent cyanine dye DiR (λEx/λEm = 748/780 nm) was used to prepare the DiR liposomes instead of miR-7. Free DiR or DiR liposomes were injected intravenously into mice. The DiR concentration was 2.5 mg/kg. The mice were placed under an in vivo imaging system at 2, 8, 24, 48, and 72 h after the injection. After taking images, the mice were sacrificed. The subcutaneous tumors, hearts, livers, spleens, lungs, kidneys, and stomachs of the mice were dissected separately and observed under the imaging system.

To visualize the liposomes in the tumor tissue under a fluorescence microscope, Cy5-miR-7 liposomes were prepared and injected into mice through the tail vein. The tumor was dissected and immediately prepared into frozen slices by a microtome (Leica). The sections were observed via a fluorescence microscope after DAPI staining.

Antitumor Effect of Liposomes in a Mouse Xenograft Model of Ovarian Cancer. We injected SKOV3 cells intraperitoneally with a cell number of 2.5×10^6 into BALB/c female nude mice to generate a mouse xenograft model of ovarian cancer. After two weeks, the tumor-bearing mice were divided randomly into three groups, each with six mice. PBS, free miR-7, and miR-7 liposomes were injected into the mice every 3 days by intravenous administration, and the dose of miR-7 was 2 mg/kg. The tumor-bearing mice were treated 7 times for 3 weeks in total. We weighed the mice every 3 days. Three days after the completion of the treatment, the mice were sacrificed. All abdominal tumors were resected and weighed. The total RNA of the tumors was immediately extracted. The level of miR-7 in the tumors was investigated via TaqMan miRNA assays. All the experiments were performed in accordance with all national or local guidelines and regulations.

Immunohistochemistry Experiment. Some of the abdominal tumors were fixed with 4% paraformaldehyde and then paraffin-embedded. We incubated the anti-EGFR antibody (1:50) with the tissue sections to detect EGFR in the tumors. The results were observed by microscopy (Leica).

Statistical Analysis. All the experiments were performed independently in triplicate. The data were presented as the mean ± standard deviation (SD). Prism 6.0 software (GraphPad) was used to analyze the data. Student's *t*-test or one-way analysis of variance (ANOVA) was performed for statistical analysis. A p value < 0.05 was defined as statistically significant.

CONCLUSIONS

Cationic liposomes provide safe and efficient drug delivery systems for the successful delivery of anticancer agents and genes. In recent years, the important role of microRNA therapy in suppressing cancer has also become a hot direction in tumor research.[12] In this work, cationic liposomes had a suitable particle size and potential and could efficiently encapsulate miR-7. The miR-7 liposomes had good tumor-targeting effects in vivo and exhibited a high transfection efficiency both in vivo and in vitro. In addition, miR-7 liposomes had a significant tumor suppressor effect in vivo, and inhibition of the EGFR pathway might be the underlying mechanism. As mentioned above, gene therapy delivered by cationic liposomes could play an important role in overcoming ovarian cancer. In the follow-up studies, we will further optimize the liposomes and target genes and strive to exert stronger anticancer effects.

AUTHOR INFORMATION

Corresponding Authors

Weiwei Feng − *Department of Obstetrics and Gynecology, Ruijin Hospital, School of Medicine, Shanghai Jiao Tong University, Shanghai 200025, China*; Phone: +86-21-64370045; Email: Fww12066@rjh.com.cn; Fax: +86-21-64370045

Wen Di − *Department of Obstetrics and Gynecology, Key Laboratory of Gynecologic Oncology, and State Key Laboratory of Oncogenes and Related Genes, Shanghai*

https://doi.org/10.1021/acsomega.1c00992
ACS Omega 2021, 6, 11669−11678

Cancer Institute, Ren Ji Hospital, School of Medicine, Shanghai Jiao Tong University, Shanghai 200127, China; orcid.org/0000-0003-4007-3856; Phone: +86-21-68383829; Email: diwen163@163.com; Fax: +86-21-68383829

Authors

Xiaojuan Cui − *Department of Obstetrics and Gynecology, Ruijin Hospital, School of Medicine and Department of Obstetrics and Gynecology, Key Laboratory of Gynecologic Oncology, and State Key Laboratory of Oncogenes and Related Genes, Shanghai Cancer Institute, Ren Ji Hospital, School of Medicine, Shanghai Jiao Tong University, Shanghai 200025, China*

Keqi Song − *Department of Obstetrics and Gynecology, Key Laboratory of Gynecologic Oncology, and State Key Laboratory of Oncogenes and Related Genes, Shanghai Cancer Institute, Ren Ji Hospital, School of Medicine, Shanghai Jiao Tong University, Shanghai 200127, China*

Xiaolan Lu − *Department of Obstetrics and Gynecology, Ruijin Hospital, School of Medicine, Shanghai Jiao Tong University, Shanghai 200025, China*

Complete contact information is available at: https://pubs.acs.org/10.1021/acsomega.1c00992

Notes

The authors declare no competing financial interest.

■ ACKNOWLEDGMENTS

The authors thank Yourong Duan of State Key Laboratory of Oncogenes and Related Genes, Shanghai Cancer Institute for technical assistance. This work was supported by the National Natural Science Foundation of China (no. 82002724) and the Research Fund of Ruijin Hospital, School of Medicine, Shanghai Jiaotong University (2019ZY03).

■ ABBREVIATIONS

MiR-7, microRNA-7; DOTAP, 1,2-dioleoyl-3-trimethylammonium-propane; DOPE, 1,2-dioleoyl-*sn*-glycero-3-phosphoethanolamine; CHOL, cholesterol; CCK-8, cell counting kit-8; DiR, 1,1′-dioctadecyl-3,3,3′,3′-tetramethylindotricarbocyanine iodide; PBS, phosphate-buffered saline; DAPI, 4′,6-diamidino-2-phenylindole; SD, standard deviation; EGFR, epidermal growth factor receptor.

■ REFERENCES

(1) Siegel, R. L.; Miller, K. D.; Jemal, A. Cancer statistics, 2020. *Ca-Cancer J. Clin.* **2020**, *70*, 7−30.

(2) Kuroki, L.; Guntupalli, S. R. Treatment of epithelial ovarian cancer. *BMJ* **2020**, *371*, m3773.

(3) Thanh Le, T.; Andreadakis, Z.; Kumar, A.; Gómez Román, R.; Tollefsen, S.; Saville, M.; Mayhew, S. The COVID-19 vaccine development landscape. *Nat. Rev. Drug Discovery* **2020**, *19*, 305−306.

(4) Amreddy, N.; Babu, A.; Muralidharan, R.; Panneerselvam, J.; Srivastava, A.; Ahmed, R.; Mehta, M.; Munshi, A.; Ramesh, R. Recent Advances in Nanoparticle-Based Cancer Drug and Gene Delivery. *Adv. Cancer Res.* **2018**, *137*, 115−170.

(5) Pan, C.-M.; Chan, K.-H.; Chen, C.-H.; Jan, C.-I.; Liu, M.-C.; Lin, C.-M.; Cho, D.-Y.; Tsai, W.-C.; Chu, Y.-T.; Cheng, C.-H.; Chuang, H.-Y.; Chiu, S.-C. MicroRNA-7 targets T-Box 2 to inhibit epithelial-mesenchymal transition and invasiveness in glioblastoma multiforme. *Cancer Lett.* **2020**, *493*, 133−142.

(6) Zhang, Z.; Zhao, M.; Wang, G. Upregulation of microRNA-7 contributes to inhibition of the growth and metastasis of osteosarcoma cells through the inhibition of IGF1R. *J. Cell. Physiol.* **2019**, *234*, 22195−22206.

(7) Kabir, T. D.; Ganda, C.; Brown, R. M.; Beveridge, D. J.; Richardson, K. L.; Chaturvedi, V.; Candy, P.; Epis, M.; Wintle, L.; Kalinowski, F.; Kopp, C.; Stuart, L. M.; Yeoh, G. C.; George, J.; Leedman, P. J. A microRNA-7/growth arrest specific 6/TYRO3 axis regulates the growth and invasiveness of sorafenib-resistant cells in human hepatocellular carcinoma. *Hepatology* **2018**, *67*, 216−231.

(8) Hu, Y.; Li, D.; Wu, A.; Qiu, X.; Di, W.; Huang, L.; Qiu, L. TWEAK-stimulated macrophages inhibit metastasis of epithelial ovarian cancer via exosomal shuttling of microRNA. *Cancer Lett.* **2017**, *393*, 60−67.

(9) Cui, X.; Sun, Y.; Shen, M.; Song, K.; Yin, X.; Di, W.; Duan, Y. Enhanced Chemotherapeutic Efficacy of Paclitaxel Nanoparticles Co-delivered with MicroRNA-7 by Inhibiting Paclitaxel-Induced EGFR/ERK pathway Activation for Ovarian Cancer Therapy. *ACS Appl. Mater. Interfaces* **2018**, *10*, 7821−7831.

(10) Chen, Y.; Zhao, H.; Tan, Z.; Zhang, C.; Fu, X. Bottleneck limitations for microRNA-based therapeutics from bench to the bedside. *Pharmazie* **2015**, *70*, 147−154.

(11) Nelson, C. E.; Robinson-Hamm, J. N.; Gersbach, C. A. Genome engineering: a new approach to gene therapy for neuromuscular disorders. *Nat. Rev. Neurol.* **2017**, *13*, 647−661.

(12) Boca, S.; Gulei, D.; Zimta, A.-A.; Onaciu, A.; Magdo, L.; Tigu, A. B.; Ionescu, C.; Irimie, A.; Buiga, R.; Berindan-Neagoe, I. Nanoscale delivery systems for microRNAs in cancer therapy. *Cell. Mol. Life Sci.* **2020**, *77*, 1059−1086.

(13) Ciani, L.; Casini, A.; Gabbiani, C.; Ristori, S.; Messori, L.; Martini, G. DOTAP/DOPE and DC-Chol/DOPE lipoplexes for gene delivery studied by circular dichroism and other biophysical techniques. *Biophys. Chem.* **2007**, *127*, 213−220.

(14) Kaddah, S.; Khreich, N.; Kaddah, F.; Charcosset, C.; Greige-Gerges, H. Cholesterol modulates the liposome membrane fluidity and permeability for a hydrophilic molecule. *Food Chem. Toxicol.* **2018**, *113*, 40−48.

(15) Hatakeyama, H.; Akita, H.; Harashima, H. A multifunctional envelope type nano device (MEND) for gene delivery to tumours based on the EPR effect: a strategy for overcoming the PEG dilemma. *Adv. Drug Delivery Rev.* **2011**, *63*, 152−160.

(16) Kozma, G. T.; Shimizu, T.; Ishida, T.; Szebeni, J. Anti-PEG antibodies: Properties, formation, testing and role in adverse immune reactions to PEGylated nano-biopharmaceuticals. *Adv. Drug Delivery Rev.* **2020**, *154-155*, 163−175.

(17) Julin, S.; Nonappa; Shen, B.; Linko, V.; Kostiainen, M. A. DNA-Origami-Templated Growth of Multilamellar Lipid Assemblies. *Angew. Chem., Int. Ed. Engl.* **2020**, *60*, DOI: DOI: 10.1002/anie.202006044.

(18) Ball, R. L.; Hajj, K. A.; Vizelman, J.; Bajaj, P.; Whitehead, K. A. Lipid Nanoparticle Formulations for Enhanced Co-delivery of siRNA and mRNA. *Nano Lett.* **2018**, *18*, 3814−3822.

(19) Harvey, R. D.; Ara, N.; Heenan, R. K.; Barlow, D. J.; Quinn, P. J.; Lawrence, M. J. Stabilization of distearoylphosphatidylcholine lamellar phases in propylene glycol using cholesterol. *Mol. Pharm.* **2013**, *10*, 4408−4417.

(20) Kim, B.-K.; Hwang, G.-B.; Seu, Y.-B.; Choi, J.-S.; Jin, K. S.; Doh, K.-O. DOTAP/DOPE ratio and cell type determine transfection efficiency with DOTAP-liposomes. *Biochim. Biophys. Acta* **2015**, *1848*, 1996−2001.

(21) Meisel, J. W.; Gokel, G. W. A Simplified Direct Lipid Mixing Lipoplex Preparation: Comparison of Liposomal-, Dimethylsulfoxide-, and Ethanol-Based Methods. *Sci. Rep.* **2016**, *6*, 27662.

(22) Ambardekar, V. V.; Han, H.-Y.; Varney, M. L.; Vinogradov, S. V.; Singh, R. K.; Vetro, J. A. The modification of siRNA with 3′ cholesterol to increase nuclease protection and suppression of native mRNA by select siRNA polyplexes. *Biomaterials* **2011**, *32*, 1404−1411.

(23) Suto, T.; Yokobori, T.; Yajima, R.; Morita, H.; Fujii, T.; Yamaguchi, S.; Altan, B.; Tsutsumi, S.; Asao, T.; Kuwano, H. MicroRNA-7expression in colorectal cancer is associated with poor

prognosis and regulates cetuximab sensitivity viaEGFR regulation. *Carcinogenesis* **2015**, *36*, 338−345.
(24) Wang, Y.; Zhou, J.; Qiu, L.; Wang, X.; Chen, L.; Liu, T.; Di, W. Cisplatin-alginate conjugate liposomes for targeted delivery to EGFR-positive ovarian cancer cells. *Biomaterials* **2014**, *35*, 4297−4309.
(25) Lv, H.; Zhang, S.; Wang, B.; Cui, S.; Yan, J. Toxicity of cationic lipids and cationic polymers in gene delivery. *J. Controlled Release* **2006**, *114*, 100−109.
(26) Rai, K.; Takigawa, N.; Ito, S.; Kashihara, H.; Ichihara, E.; Yasuda, T.; Shimizu, K.; Tanimoto, M.; Kiura, K. Liposomal delivery of MicroRNA-7-expressing plasmid overcomes epidermal growth factor receptor tyrosine kinase inhibitor-resistance in lung cancer cells. *Mol. Cancer Ther.* **2011**, *10*, 1720−1727.
(27) Cui, Y.-X.; Bradbury, R.; Flamini, V.; Wu, B.; Jordan, N.; Jiang, W. G. MicroRNA-7 suppresses the homing and migration potential of human endothelial cells to highly metastatic human breast cancer cells. *Br. J. Cancer* **2017**, *117*, 89−101.
(28) Shao, G.; Wang, R.; Sun, A.; Wei, J.; Peng, K.; Dai, Q.; Yang, W.; Lin, Q. The E3 ubiquitin ligase NEDD4 mediates cell migration signaling of EGFR in lung cancer cells. *Mol. Cancer* **2018**, *17*, 24.
(29) Hu, W.; Zheng, S.; Guo, H.; Dai, B.; Ni, J.; Shi, Y.; Bian, H.; Li, L.; Shen, Y.; Wu, M.; Tian, Z.; Liu, G.; Hossain, M. A.; Yang, H.; Wang, D.; Zhang, Q.; Yu, J.; Birnbaumer, L.; Feng, J.; Yu, D.; Yang, Y. PLAGL2-EGFR-HIF-1/2α Signaling Loop Promotes HCC Progression and Erlotinib Insensitivity. *Hepatology* **2021**, *73*, 674.
(30) Gu, Y.; Zhang, S. High-throughput sequencing identification of differentially expressed microRNAs in metastatic ovarian cancer with experimental validations. *Cancer Cell Int.* **2020**, *20*, 517.
(31) Nakamura, H.; Jun, F.; Maeda, H. Development of next-generation macromolecular drugs based on the EPR effect: challenges and pitfalls. *Expert Opin. Drug Delivery* **2015**, *12*, 53−64.
(32) Sindhwani, S.; Syed, A. M.; Ngai, J.; Kingston, B. R.; Maiorino, L.; Rothschild, J.; MacMillan, P.; Zhang, Y.; Rajesh, N. U.; Hoang, T.; Wu, J. L. Y.; Wilhelm, S.; Zilman, A.; Gadde, S.; Sulaiman, A.; Ouyang, B.; Lin, Z.; Wang, L.; Egeblad, M.; Chan, W. C. W. The entry of nanoparticles into solid tumours. *Nat. Mater.* **2020**, *19*, 566−575.
(33) Pandit, S.; Dutta, D.; Nie, S. Active transcytosis and new opportunities for cancer nanomedicine. *Nat. Mater.* **2020**, *19*, 478−480.
(34) Zhou, Q.; Shao, S.; Wang, J.; Xu, C.; Xiang, J.; Piao, Y.; Zhou, Z.; Yu, Q.; Tang, J.; Liu, X.; Gan, Z.; Mo, R.; Gu, Z.; Shen, Y. Enzyme-activatable polymer-drug conjugate augments tumour penetration and treatment efficacy. *Nat. Nanotechnol.* **2019**, *14*, 799−809.
(35) Pan, M.; Li, M.; You, C.; Zhao, F.; Guo, M.; Xu, H.; Li, L.; Wang, L.; Dou, J. Inhibition of breast cancer growth via miR-7 suppressing ALDH1A3 activity concomitant with decreasing breast cancer stem cell subpopulation. *J. Cell. Physiol.* **2020**, *235*, 1405−1416.
(36) Filipczak, N.; Pan, J.; Yalamarty, S. S. K.; Torchilin, V. P. Recent advancements in liposome technology. *Adv. Drug Delivery Rev.* **2020**, *156*, 4−22.

https://doi.org/10.1021/acsomega.1c00992
ACS Omega 2021, 6, 11669−11678